Journal of Catalysis **194,** 105–114 (2000)
doi:10.1006/jcat.2000.2908, available online at http://www.idealibrary.com on IDEAL®

On the Induction Period of Methane Aromatization over Mo-Based Catalysts

Ding Ma, Yuying Shu, Mojie Cheng, Yide Xu, and Xinhe Bao[1]

State Key Laboratory of Catalysis, Dalian Institute of Chemical Physics, Chinese Academy of Sciences, 457 Zhongshan Road, P.O. Box 110, Dalian 116023, China

Received February 7, 2000; revised April 26, 2000; accepted April 27, 2000

The behavior of different species during the temperature-programmed surface reaction (TPSR) of methane over various catalysts is traced by an online mass spectrometer. It is demonstrated that the transformation of MoO_3 to molybdenum carbide hinders the activation of methane as well as the succeeding aromatization in the TPSR. If this transformation process is done before the reaction, the temperature needed for methane activation and benzene formation will be greatly lowered (760 and 847 K, respectively). On the basis of comparison of the catalytic behavior of molybdenum supported on different zeolites, it is suggested that the initial activation of methane is the rate-determining step of this reaction. For the cobalt catalysts supported on HMCM-22 or Mo catalysts supported on TiO_2, no benzene formation could be observed during the TPSR. However, the prohibition of benzene formation is different in nature over these two catalysts: the former lacks the special properties exhibited by molybdenum carbide, which can continuously activate methane even when multiple layers of carbonaceous species are formed on its surface, while the latter cannot accomplish the aromatization reaction since there are no Brønsted acid sites to which the activated intermediates can migrate, although the activation of methane can be achieved on it. Only for the catalysts that possess both of these properties, together with the special channel structure of zeolite, can efficient methane aromatization be accomplished.

Key Words: **methane dehydroaromatization; induction period; molybdenum carbide; MCM-22; ZSM-5; TPSR.**

INTRODUCTION

Direct conversion of methane to useful industrial products has attracted increasing attention in past century, especially in the past decade (1). Different approaches have been developed in order to get a better and efficient utilization of natural gas, such as two-step transformation of methane into C2 hydrocarbons over Pt or Ru catalysts (2, 3) and selective oxidation of methane to methanol (4). However, it is still impractical to put most of these methods into industrial use due to their relatively low yields and poor selectivities. It is significant that methane can be converted into benzene under nonoxidative conditions over Mo/HZSM-5 (5), and this process can be regarded as an analogy to propane or ethane aromatization over Ga/Zn-modified HZSM-5 catalysts (6). Recently, the reaction mechanism (7–9), the location of loaded TMI (10–12), the coupled reaction (13), etc., have been extensively investigated by various authors. It is verified that a smooth running of the reaction requires proper cooperation between the Brønsted acid sites and the molybdenum species (12). Besides, there is an induction period before the aromatization occurs. The induction period has been attributed to the conversion of MoO_3 into Mo_2C under the action of the methane reactant. Also, it is believed that the Mo_2C phase is responsible for the activation of methane (8, 14). Borry *et al.* (15) proposed the structure of the active sites on the basis of the investigation of water desorption during catalyst preparation and on the basis of isotopic exchange experiments. However, little attention has been paid to what happens during the induction period other than the changes of the molybdenum, and where and how carbonaceous deposition occurs. Recently, we have reported that better catalytic performance of this reaction can be achieved on a molybdenum catalyst supported on HMCM-22 (16). This catalyst gives a higher benzene selectivity and has a longer lifetime when compared with Mo/HZSM-5. Consequently, it becomes possible to investigate the above-mentioned questions by comparison of different catalyst systems. In this paper, we report detailed studies of these issues over zeolite-supported or oxide-supported molybdenum or cobalt catalysts by TPSR-MS, TPO, XPS, etc. The variation of different products was traced, and the nature of the induction period as well as the environment needed for methane aromatization are revealed and discussed.

EXPERIMENTAL

Catalysts Preparation and Evaluation

MCM-22 zeolite (Si/Al = 15) was synthesized according to the procedures described in the references, using

[1] To whom correspondence should be addressed. Fax: 0086-411-4694447. E-mail: xhbao@ms.dicp.ac.cn.

0021-9517/00 $35.00

hexamethyleneimine (HMI) as the directing agent (17, 18). The details of the synthesis have been given elsewhere (16). Mo/HMCM-22 catalysts containing 2–10% Mo were prepared by impregnating 10 g of HMCM-22 powder with 20 ml of aqueous solution which contained the desired amount of ammonium heptamolybdate (AHM), then dried at room temperature for 12 h. After further drying at 373 K for 8 h and calcining in air at 773 K for 5 h, the samples were crushed and sieved to 20–60 mesh granules for catalytic evaluations. Hereafter, the Mo/HMCM-22 catalysts with different Mo loading will be denoted as *x*Mo/HMCM-22, where *x* is the nominal Mo content in weight percent. The preparation of the 6% Mo/HZSM-5 (HZSM-5 was provided by Nan Kai University, with Si/Al = 25), 6% Mo/TiO_2, and 3.7% Co/HMCM-22 catalysts were carried out by similar procedures, and they are denoted as 6Mo/HZSM-5, 6Mo/TiO_2 and 3.7Co/HMCM-22, respectively. The texture and chemical properties of these catalysts (surface area, etc.) have been given in Refs. (11, 12, and 16).

The reaction was carried out in a 6.2-mm-i.d. quartz tubular fixed-bed reactor. The products were analyzed by an online gas chromatograph (Shimadzu GC-9A) equipped with a flame ionization detector (FID) using an OV-101 6201 column, and a thermal conductivity detector (TCD) using a HayeSep-D column. The reaction rates were expressed in nanomoles of methane per gram per second. In order to determine the coke formation rate, 9.5% N_2 was added in methane as an internal standard. The formation rates of the products were calculated from the amount of methane consumed. Details were presented elsewhere (11).

Temperature Programming Experiments

A TP-MS apparatus was built to conduct transient experiments such as TPSR (temperature-programmed surface reaction), TPR (temperature-programmed reduction), TPO (temperature-programmed oxidation), pulse adsorption, and pulse reaction. It consists of an outdoor gas cylinder station, a gas flow control unit, a U-shaped reactor, and a detector (see Fig. 1). Before entering the reactor, the gases were passed through a water trap and an oxygen trap (except for O_2/He) for further purification, and the gas flows were adjusted by a mass flow controller (Jian Zhong, D08-4A/ZM).

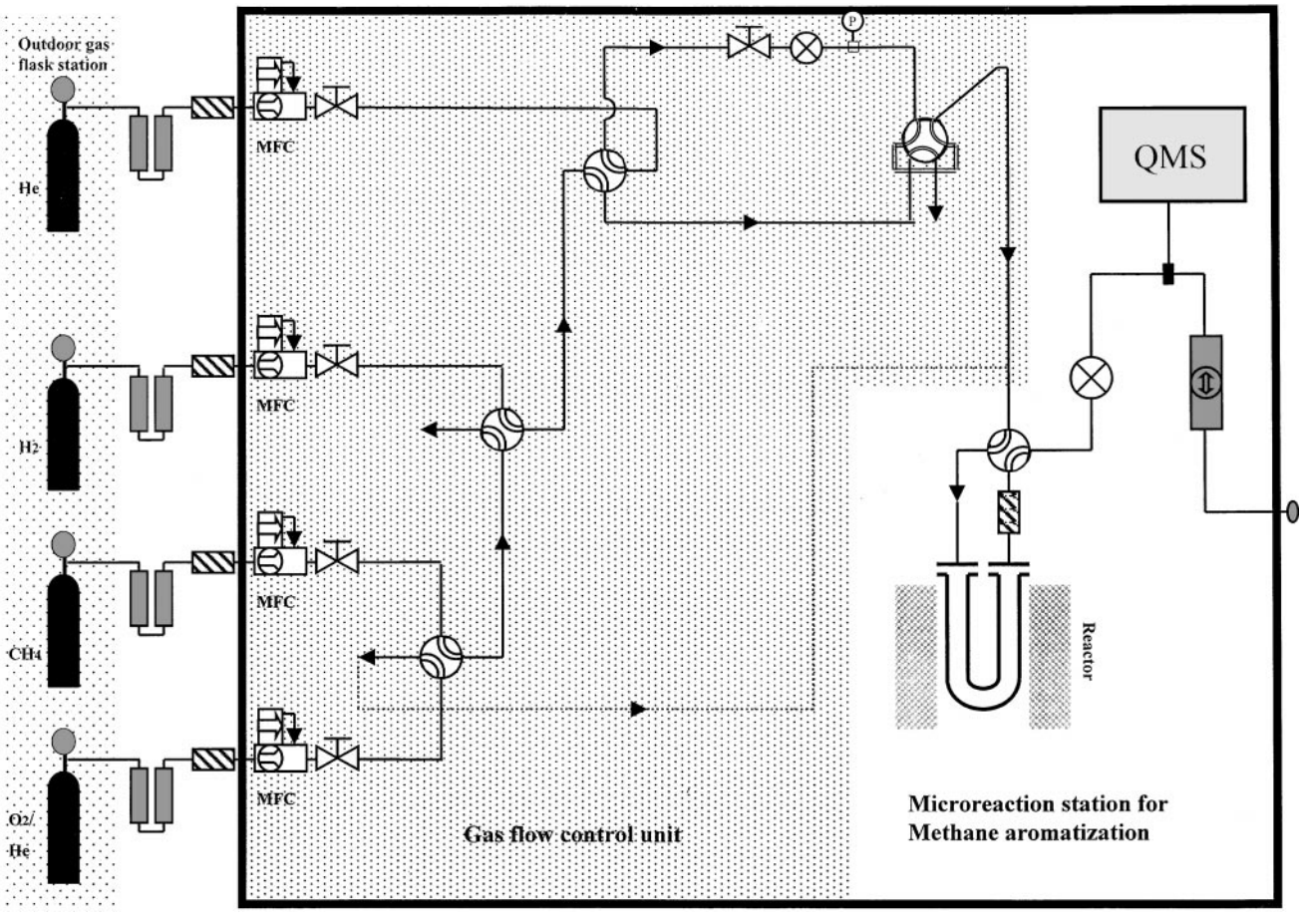

FIG. 1. Scheme of the apparatus for various kinds of temperature-programmed studies, such as TPSR, TPO, and TPH. The variation of different species is monitored by an online mass spectrometer, which could detect 64 mass numbers at the same time. MFC, mass flow controller.

By means of 3 four-way valves and a six-way valve, the gas entering the reactor could be smoothly switched among all four kinds of gases. The reaction products/desorption products were analyzed by an online quadruple mass spectrometer (Balzers, QMS 200) equipped with a computer interface. The QMS was capable of measuring mass spectral intensities for a maximum of 64 preselected masses as a function of time or temperature.

In the present study, the catalyst (150 mg) was placed near the bottom of the reactor. For TPSR, the catalyst was first heated under an He stream (30 ml/min) to 873 K (10 K/min) and kept at this temperature for 40 min to remove the adsorbed water. After being cooled to RT, the sample was flushed with methane (99.99%, 7.5 ml/min) at the same temperature for 1 h. Then, TPSR was conducted from 293 to 1095 K at a heating rate of 5 K/min. The product gases leaving the reactor were analyzed by the mass spectrometer through a capillary. During the temperature ramp, MS intensities for 2 (H_2), 15, 16 (CH_4), 18 (H_2O), 27 (C_2H_4), 28 (CO), 30 (C_2H_6), 44 (CO_2), and 78 (C_6H_6) were measured as a function of temperature. Mass number 27 was chosen for ethene to distinguish it from that of CO (28); however, the donation of ethene to mass number 28 has been subtracted with careful calibration. For some TPSR experiments, 6MoHMCM-22 or 6MoHZSM-5 was prereduced in H_2 (60 ml/min) at 973 K for 3 h, or carburized in a CH_4/H_2 (75 ml/min, with mole ratio of 1/4) stream at 973 K for 3 h to get the molybdenum carbide catalysts. After cooling to RT, the remaining gases were swept by methane (99.99%, 7.5 ml/min) at RT before the TPSR. TPO was performed after the catalyst had undergone 3 h of reaction and been cooled in an identical atmosphere, and was flushed with a 10% O_2/He mixture (20 ml/min) at RT for 1 h. The temperature was raised from 303 to 1023 K at a rate of 8 K/min. The mass intensities for 32 (O_2) and 44 (CO_2) were recorded.

All gases used were in UHV grade.

XPS Spectroscopy

XPS measurements were performed in a modified Leybold LHS 12 MCD system equipped with facilities for UPS (He I, 21.22 eV; He II, 40.8 eV) and XPS (Mg K, 1253.6 eV, 240 W power). The base pressure was lower than 1×10^{-10} mbar. All binding energies were referenced to the zeolitic Al 2*p* and Si 2*p* peaks at 74.5 and 102.8 eV, respectively. The XPS of fresh 6Mo/HMCM-22 and that after reaction were accumulated for five scans each. After reaction, the catalyst was cooled in a methane atmosphere before being transferred into the XPS system.

RESULTS AND DISCUSSION

Catalytic Results

The performances of the Mo/HMCM-22, Mo/HZSM-5, Mo/TiO_2, and Co/HMCM-22 catalysts are summarized in Table 1. As is well known, MCM-22, which possesses two kinds of channel structures, exhibits the behavior of both 10MR and 12MR systems (18–20). Its topological structure, as suggested by Leonowicz *et al.* (19), is composed of interconnected $\{4^3 5^6 6^3 [4^3]\}$ building units forming two independent pore systems: two-dimensional, sinusoidal, 10-ring intralayer channels and 12-ring interlayer supercages with a depth of 18.2 Å, both accessible through 10-ring apertures. Recently, we have reported (16) a catalyst supported on MCM-22, which gave a better catalytic performance in methane dehydroaromatization as compared with that of Mo/HZSM-5, i.e., a higher benzene selectivity (>80% in maximum) and a longer lifetime (more than 24 h at benzene yield higher than 6%). As shown in Table 1, the methane-depleting rate of the 6Mo/HZSM-5 and the 6Mo/HMCM-22 are similar, but the latter gave a larger amount of benzene at the expense of naphthalene formation. Moreover, the longer lifetime of the Mo/HMCM-22 indicates that it probably has a stronger ability to accommodate more carbonaceous deposits as compared with the Mo/HZSM-5, since the Mo/HMCM-22 showed a comparable or higher coke formation rate in all the periods investigated. These behaviors could be attributed to the unique structure of MCM-22, namely, it has a 12MR pocket in both the external surface and the internal channel, which may accommodate more coke and naphthalene; the latter in end may suppress naphthalene formation. However, the Mo/HMCM-22 also shows typical behaviors which are exhibited by various Mo-based zeolites for methane aromatization, such as the existence of an induction period in the reaction and the transformation of MoO_3 into molybdenum carbide during the induction period, etc. Untill now, Mo/HMCM-22 and Mo/HZSM-5 have been the best catalysts for methane aromatization among Mo-based catalysts. Thus, the Mo/HMCM-22 provides us with an alternative system to compare and investigate the above-mentioned issues. In addition, Mo/TiO_2 and Co/HMCM-22 were chosen because both of them give only small amounts of CO and CO_2, along with the formation of coke in the reaction, but no formation of aromatics is observed. This is probably

TABLE 1

Catalytic Performances of Various Catalysts (the Formation Rates of Products Are Based on Consumed Methane)[a]

	Depleting rate or formation rate of (nmol/g · s)						
	CH_4	CO	C_2	C_6H_6	C_7H_8	$C_{10}H_8$	Coke
6Mo/HZSM-5	1673.3	11.8	62.3	947.7	43.8	304.7	276.1
6Mo/HMCM-22	1780.4	8.4	48.8	1188.8	47.1	101.0	336.7
6Mo/TiO_2	296.3	15.2					281.1
3.7Co/HMCM-22	301.3	3.4					297.9

[a] Data were taken after the reaction was run for 120 min (SV = 1500 ml/g · h, $T = 973$ K).

due to the fact that the Mo/TiO_2 catalyst lacks strong acidity, while the Co/HMCM-22 is not a Mo-based catalyst. Mo/SiO_2 is not a suitable catalyst for the present investigation, since it gives a small amount of benzene in this reaction, which may result from the acidity originating from the aluminum impurity in the support.

TPSR-MS of Mo/HMCM-22 with Various Mo Loadings

The formation of various products during the temperature-programmed surface reaction of methane over the Mo/HMCM-22 is illustrated in Figs. 2–4. In Fig. 2, the variation of methane, hydrogen, and carbon monoxide is drawn in the upper frame, while that of water, ethene, carbon dioxide, and benzene is demonstrated in the lower part. It should be noted that they were drawn with two different scales, and the fluctuation of the line is due to the instability of the MS. Below 800 K no apparent consumption of methane or formation of any products can be observed, which indicates that methane cannot be activated over zeolite-supported molybdenum catalysts below 800 K, and this is consistent with our previous results (5). Above

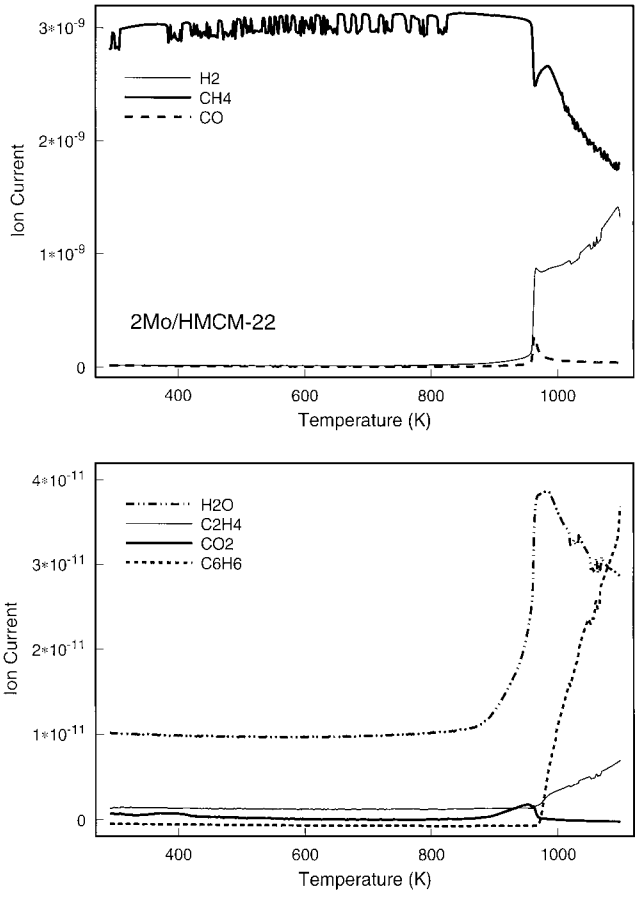

FIG. 2. TPSR profiles over the 2Mo/HMCM-22 catalyst. Methane flow rate, 7.5 ml/min; heating rate, 5 K/min. Notice the upper and the bottom profiles are drawn with different scales.

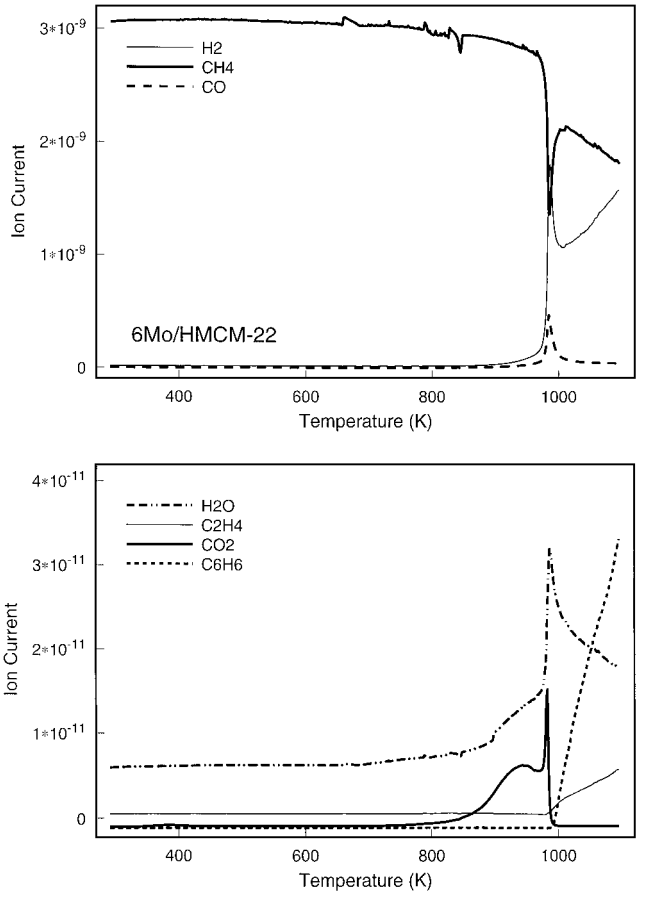

FIG. 3. TPSR profiles over the 6Mo/HMCM-22 catalyst.

820 K, there is a small methane consumption, accompanied by the formation of CO_2 and H_2O. Meanwhile, no apparent formation of other products such as ethene, CO, or H_2 was observed. The production of CO_2 increased gradually with the increase of temperature, and passed a maximum at 950 K. Then, a sharp increase in formation of the H_2 and CO is observed concurrently with a sharp depletion of methane. The amount of methane consumed is so large that an inverse peak is formed. It is interesting to note that the peak maxima of methane, H_2, and CO are at the same temperature (963 K). And after that, the consumption of methane and the production of H_2 continued, while that of CO and CO_2 gradually ceased. Meanwhile, a dramatic change occurred; i.e., the formation of benzene and ethene could be clearly observed (969 K). Both of them increased with the temperature until the end of the TPSR. The gradually increasing consumption of methane is detected simultaneously with the further formation of hydrogen. By increasing the Mo loading, a similar feature could be observed (Figs. 3 and 4), but all the peaks shifted to a higher temperature, e.g., those of CO_2 and CH_4 shifted to 940 K and 984 K, respectively (Fig. 3). Similarly, the formation of benzene and ethene is also delayed (992 K).

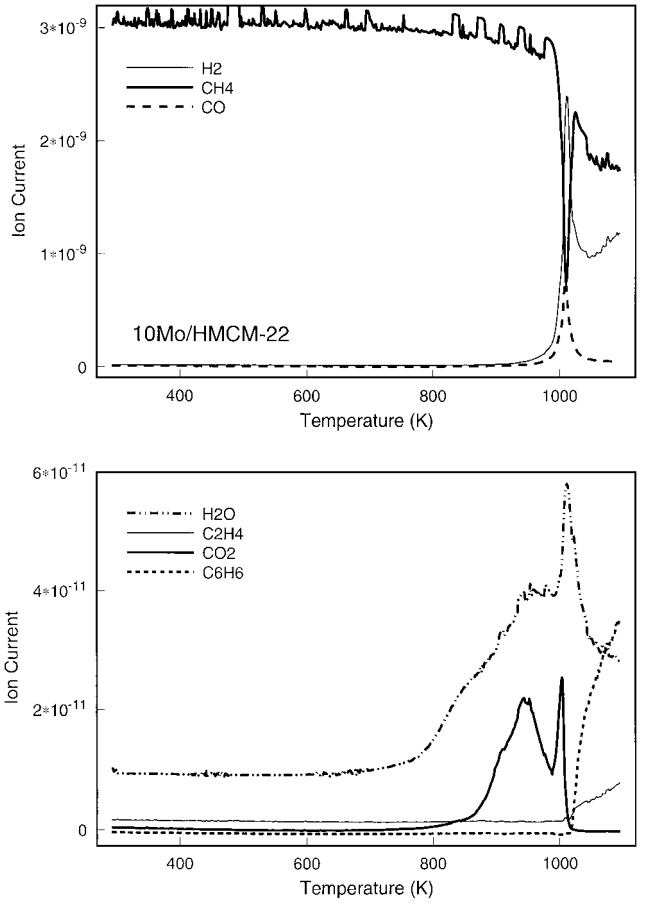

FIG. 4. TPSR profiles over the 10Mo/HMCM-22 catalyst.

The temperature for the maximum formation of CO and H_2 is identical with that of the depletion of methane. We notice that the line of CO_2 splits into a double peak located at 939 and 982 K, respectively (Fig. 3), and the peak temperature of the latter is consistent with that of CO and H_2. In fact, for 2MoHMCM-22, a double peak structure of CO_2 can also be resolved if a smaller temperature scale is chosen. The temperature of the second peak is also the same as that of CO and H_2 over the 2MoHMCM-22.

Thus, in the TPSR of the methane over Mo/HMCM-22, three reaction regions could be identified. The first one is from about 820 to 960 K. In this region, the main products are CO_2 and H_2O, and no apparent formation of H_2 and CO could be observed. After that, a sharp consumption of methane accompanied with a sharp formation of CO, H_2, CO_2, and H_2O occurred (second region). Only at almost the end of CO_2 production could benzene formation occur (third region). The TPSR over the 10Mo/HMCM-22 and the 6Mo/HZSM-5 has also verified this observation (see Figs. 4 and 8). The depletion of methane and the release of H_2 increased with the increase in the formation of benzene and ethene. The first two stages could be taken as the induction period of the reaction, which had been reported by Lunsford *et al.* (8) and Solymosi *et al.* (14) on the Mo/HZSM-5 catalyst. They suggested that the induction period observed comes from the transformation of MoO_3 into Mo_2C species. In the present case, we believe that the first two steps correspond to the formation of Mo_2C. As reported by Lee *et al.* (21), during the transformation of MoO_3 into Mo_2C over supported or unsupported MoO_3 catalysts, a two-step process occurs. The first is the reduction of MoO_3 to MoO_2, then followed by the carburization of MoO_2 into molybdenum carbide. The production of H_2O and CO_2 could be detected in both processes, whereas that of H_2 is observed only in the latter process (CO not measured). This is in good agreement with our present results, and the first and second steps correspond respectively to the formation of the MoO_2 and the molybdenum carbide. The existence of Mo_2C was checked by XPS, using a fresh 6Mo/HMCM-22 catalyst which has been run in a temperature-programmed surface reaction to about 1000 K, when the initial benzene formation happened. As shown in Fig. 5, the fresh 6Mo/HMCM-22 presents a typical Mo 3*d* doublet at 235.6 and 232.8 eV, respectively. It is consistent with those reported previously on fresh

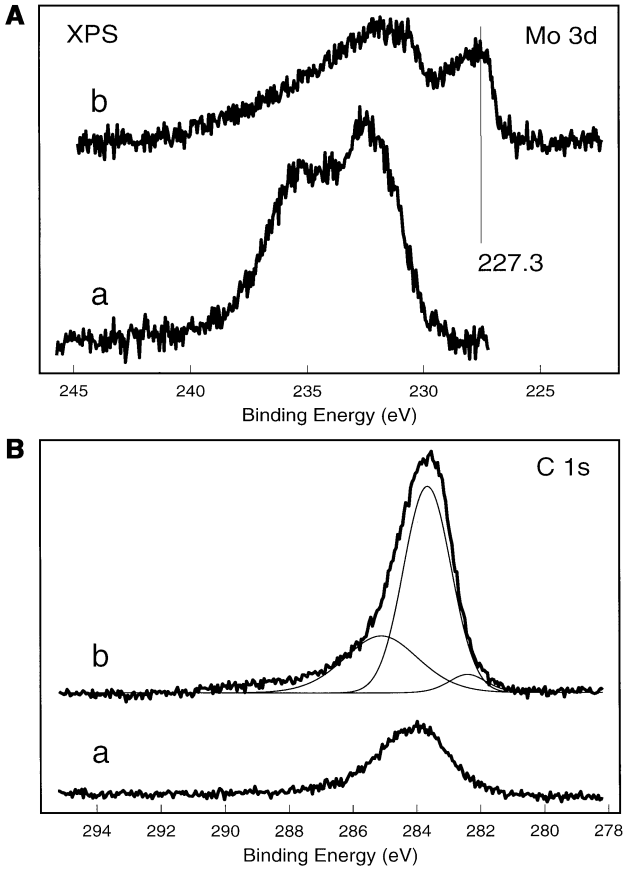

FIG. 5. XPS spectra of (A) the Mo 3*d* region, and (B) the C 1s region of (a) fresh 6Mo/HMCM-22, and (b) 6Mo/HMCM-22 after temperature-programmed reaction up to about 1000 K.

Mo/HZSM-5. In the C 1*s* region, the appearance of a symmetric peak at about 284.0 eV is due to the carbon pollution in the vacuum system. When the catalyst had undergone TPSR up to about 1000 K, the transformation of Mo oxide to molybdenum carbide happened. The binding energy of the Mo ($3d_{5/2}$) was 227.5 eV, which agreed well with the value reported by various authors for Mo_2C produced from MoO_3/HZSM-5 during the conversion of methane into benzene (22, 23), as well as that of pure Mo_2C and Al_2O_3 supported Mo_2C (24). On the other hand, the C 1*s* peak increased and broadened, which indicates that carbon deposition occurred, and the carbon deposits are represented by peaks with different binding energies that may be attributed to different kinds of C in the surface of the catalysts. By deconvolution, three peaks can be found in the C 1*s* region, which is consistent with the observation of Lunsford and co-workers by the angle-resolved XPS technique (22). The first two steps of this reaction can be illustrated as follows:

$$MoO_3 + CH_4 \rightarrow MoO_2 + CO_2 + H_2O \quad [1]$$

$$MoO_2 + CH_4 \rightarrow Mo_2C + CO + H_2 + CO_2 + H_2O. \quad [2]$$

The second step is a more vigorous reaction as compared with the first one. It occurred in a relatively narrow temperature range, and to a certain degree it is just like a phase transformation.

It should be noted that the peak areas of CO_2 and CO, which represent the amount of the Mo_2C species produced, increased with the increase of Mo loading. This further supported our conclusion that the first two steps correspond to MoO_3 reduction and Mo_2C formation, as they are stoichiometric reactions. The increase in peak temperature of all the species in the first two steps indicates that the interaction between the molybdenum oxide and the zeolite varied with the increase of Mo loading. Perhaps there are larger particles in the case of high Mo loading catalysts, which are more difficult to reduce/react, which thus leads to the increase in temperature of these peaks. The rising of the benzene formation curve demonstrates that the reaction is accelerated by temperature increases.

TPSR of 6Mo/HMCM-22 after Reduction or Carburization

Upon reduction at 973 K with flowing hydrogen (60 ml/min) for 3 h, the TPSR profile of the 6MoHMCM-22 presents a behavior similar to that of the fresh catalyst (Fig. 6). The three steps could be well observed, but the intensities of the former two shrank, while at the same time the peak temperature became lower. The production of benzene can be observed much earlier (955 K) as a result of the quicker ending of the formation of the CO_2, which indicates that the transformation of MoO_3 to Mo_2C is easier on the hydrogen-reduced catalysts. But as reported previously, even zeolite-supported metal molybdenum needs to be carburized during the reaction (14), which implies

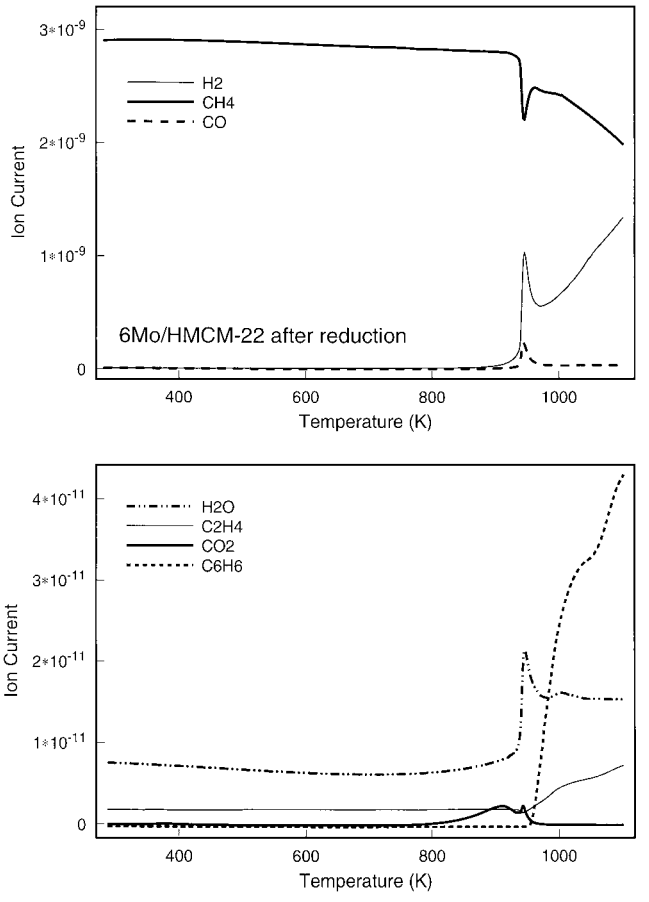

FIG. 6. TPSR profiles over the 6Mo/HMCM-22 catalyst after reduction in flowing H_2 (60 ml/min) at 973 K for 3 h. Before TPSR, the catalyst was swept by methane at RT for 1 h.

that the reduction process could not remove the induction period.

However, after treating with 20% CH_4/H_2 (75 ml/min) at 973 K for 3 h, a dramatic change occurred. As shown in Fig. 7, the above-mentioned first two steps disappeared, while the activation of methane could be observed as early as at 760 K, and the formation of benzene and ethene appeared at 847 K. It is well known that high-temperature treatment with 20% CH_4/H_2 will lead to the transformation of MoO_3 into Mo_2C (21), which has also been taken as a routine method for preparing unsupported or supported molybdenum carbide. Thus, this demonstrated that the activation of methane as well as the production of benzene could be conducted at a much lower temperature. Lunsford *et al.* (8) and we (25) had suggested that ethene or something similar is the intermediate of this reaction, whereas some of the authors pointed out that it is acetylene which is the primary product (26). However, both of these substances are easily (could be initiated lower than 673 K) aromatized on a zeolite that possesses Brønsted acidity. And it is generally accepted that it is the cleavage of the C–H bond of methane that is the rate-determining step in many

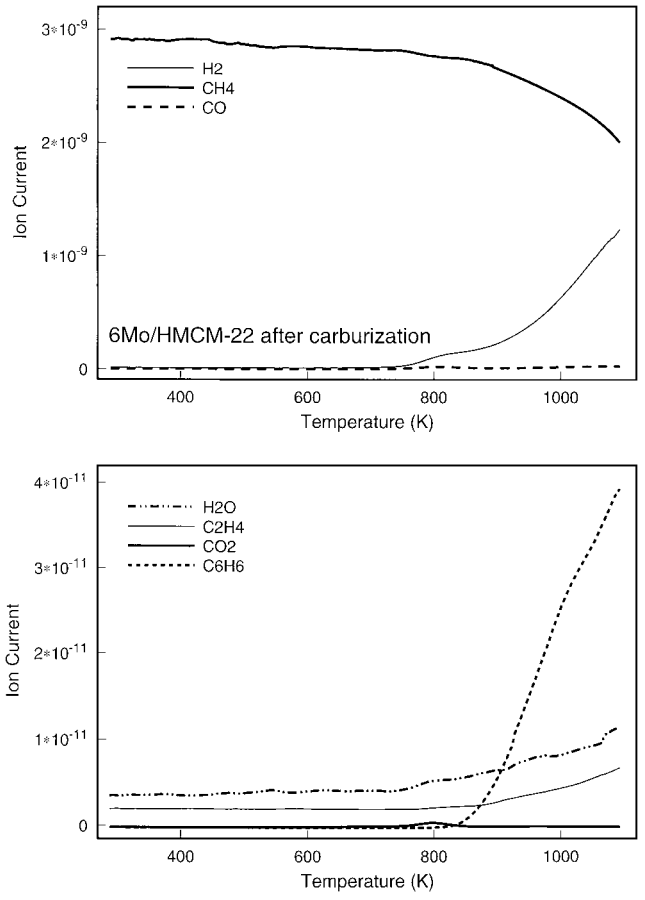

FIG. 7. TPSR profiles over the 6Mo/HMCM-22 catalyst after treatment in 20% CH_4/H_2 (75 ml/min) at 973 K for 3 h. Before TPSR, the $6Mo_2C$/HMCM-22 was swept by methane at RT for 1 h.

methane transformation reactions (1). Thereafter, if an active center for methane activation is formed, the transformation will be easy to carry out. Our present situation is just that case, and it is the first two steps (formulas [1] and [2]) that hinder the activation and aromatization of methane, so that benzene formation can be observed only at a relatively high temperature. If these barriers are eliminated before the TPSR, the temperature for benzene production will be greatly lowered (in the present case, 847 K). However, the conversion is governed by thermodynamic limits.

Lunsford *et al.* (8) had observed the existence of the induction period under the condition that an MoO_3/HZSM-5 had been carburized in CH_4/H_2 atmosphere for as long as 16 h. They attributed this to the fact that a clean surface of Mo_2C is too reactive to form a higher hydrocarbon. But it is important to notice that the initial products of their aromatization reaction on Mo_2C/HZSM still contained large amount of CO (about 40% of that of MoO_3/HZSM-5). In fact, in the present case, we could still observe a weak peak of CO_2/CO between the activation of methane (760 K, judging by the release of H_2) and the formation of benzene (847 K). It is well known that fresh molybdenum carbide or nitride is very active and will spontaneously combust when exposed to air (27). Thus, it is not difficult to imagine that it will react with a trace amount of oxygen contained in CH_4 during the 1 h flushing before TPSR. Therefore, the molybdenum carbide may be oxidized, leading to the production of CO_2/CO during the TPSR-MS and to the recarburization into pure molybdenum carbide. We believe that if oxygen was fully/strictly eliminated, we would observe the simultaneous activation of methane and the formation of benzene at a lower temperature. However, it is difficult to realize such a strict condition. Also, perhaps a period of time for the accumulation of carbon species in order to yield primary products is necessary, but it may differ from the site-blocking effect (8).

The TPSR profiles of the fresh and carburized 6Mo/HZSM-5 catalysts are shown in Figs. 8a and 8b, and both of them are similar to the corresponding profiles of the 6Mo/HMCM-22. The temperature for benzene formation is 40 K lower for the fresh 6Mo/HZSM-5 with respect to the fresh 6Mo/HMCM-22, which suggests that the effects of these two kinds of supports on the dispersion of molybdenum oxide may differ. However, after carburization, it is interesting to note that a nearly similar initial formation temperature for benzene is observed on the two catalysts (847 and 861 K). This strongly argues our conclusion that the initial activation of methane is the key step in the whole reaction, and it is the formation of the active centers that hinders the formation of benzene.

TPSR of 6Mo/TiO_2 and 3.7Co/HMCM-22

Both of these catalysts show zero benzene formation in catalytic evaluation (Table 1). It is worth pointing out that the former catalyst contains molybdenum but lacks Brønsted acid sites for the aromatization of the intermediates, while the latter catalyst has Brønsted sites, but is scant of active species, although cobalt itself can also form a cobalt carbide (27). The TPSR profiles of the 6Mo/TiO_2 and 3.7Co/HMCM-22 are illustrated in Figs. 9 and 10. As shown in Fig. 9, the first two steps for the activation of methane can be clearly observed in the TiO_2-supported catalyst, but after about 1000 K, i.e., after the end of the formation of CO_2, no benzene formation is detected, although the depletion of methane and the release of H_2 continued. We had scanned the mass number from 2 to 150 during this period, but no formation of other products was observed except for the release of H_2 and a small amount of water. However, consumption of methane did occur, as demonstrated in Fig. 9. Thus, we concluded that the consumed methane has deposited on the surface of the catalyst with the release of hydrogen. Since there is no existence of Brønsted acid sites that are responsible for intermediate aromatization, no benzene formation could be found. In other words, the activated species (cannot be clearly described at the present time)

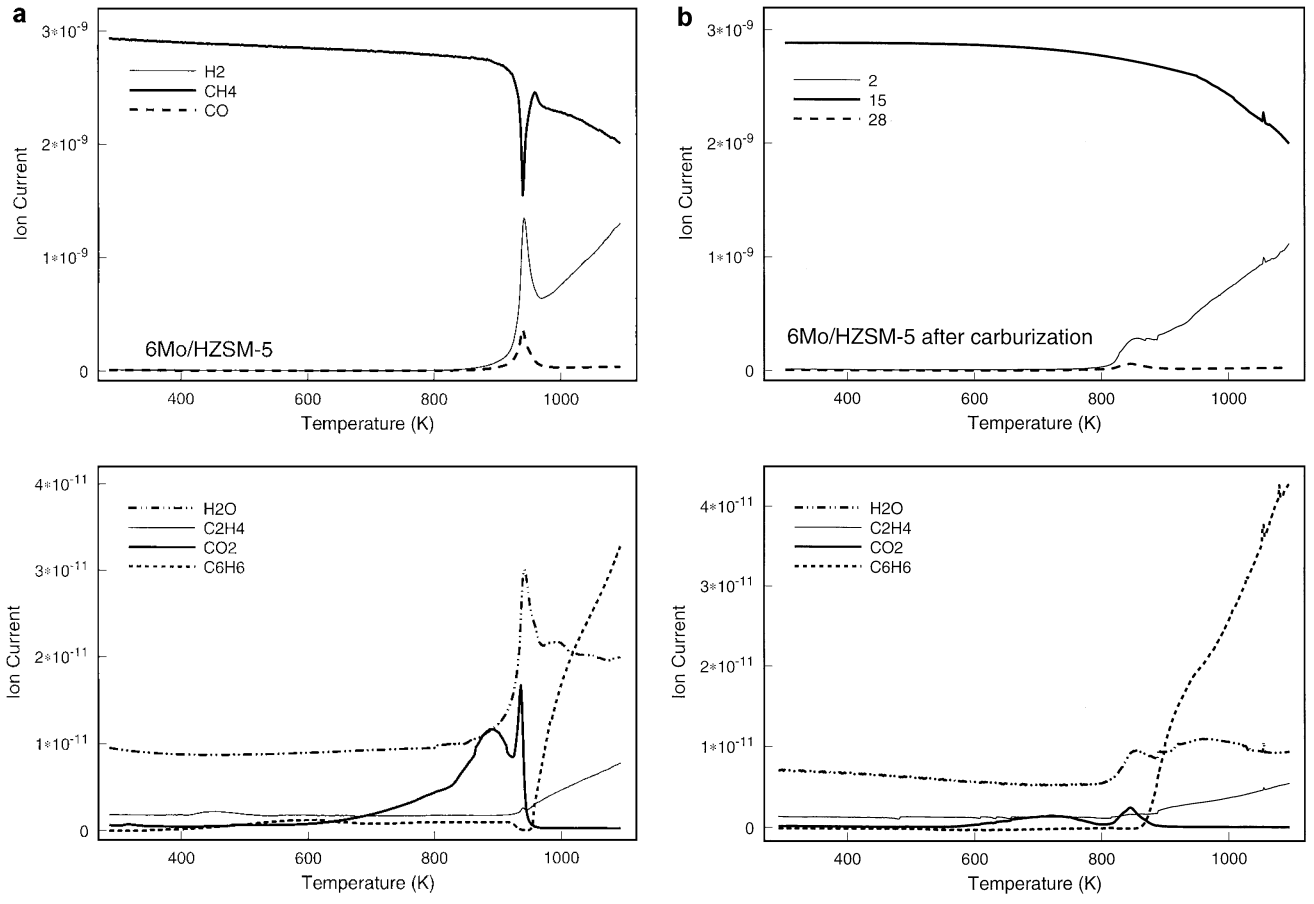

FIG. 8. TPSR profiles over the 6Mo/HZSM-5 catalyst before (a) and after (b) treatment in 20% CH_4/H_2 (75 ml/min) at 973 K for 3 h.

cannot efficiently migrate to the acid sites to accomplish aromatization (since there are no such sites), although methane can be continuously activated. As suggested earlier, ethene is the primary product of this reaction and it is produced by the molybdenum species. However, it must be noted that no apparent formation of ethene and ethane is observed after Mo_2C is formed. This indicates that the formation of ethene must be assisted by Brønsted sites, i.e., a kind of acid-assisted formation. Or, this may imply that ethene is not the intermediate species, whereas the carbon pool of the catalyst surface (7), created as the result of continuous activation of methane, may be responsible for the methane aromatization. Regarding this aspect, further investigation is needed.

The TPSR of the 3.7Co/HMCM-22 catalyst presents a different picture (see Fig. 10). The transformation of cobalt oxide into cobalt carbide had been reported previously, and in the present case, we believe that the appearance of the peaks of H_2, CH_4, CO, etc. can be attributed to this transformation. However, after the transformation, one cannot observe any apparent consumption of methane, let alone benzene formation. Although this catalyst has Brønsted acid sites, but owing to the poor ability of cobalt or cobalt carbide to activate methane, no hydrocarbon products are observed (notice that there is an extremely small amount of ethene at high temperature, which may result from the thermal reaction of methane at this temperature, but the amount is so small that it cannot result in the formation of benzene).

TPO of 6Mo/TiO_2 and 6Mo/HMCM-22 after Reaction at 973 K for 3 h

TPO is an efficient method for the characterization of the content as well as for the distinguishing of different kinds of coke species (28). Here, we demonstrate the TPO profiles of the 6Mo/TiO_2 and the 6Mo/HMCM-22 after reaction at 973 K for 3 h (Fig. 11). The consumption of oxygen is also drawn on a specific figure, and it is consistent with the production of CO_2. As shown in Fig. 11, the 6Mo/HMCM-22 gives a doublet peak located at 742 and 830 K, respectively. Two kinds of coke-burning behavior could also be observed in the TG study. This indicates that at least two kinds of coke exist on the catalyst surface, and this is in good agreement with the results of XPS over coked Mo/HZSM-5 catalysts. It is believed that deactivation of this kind of catalysts is

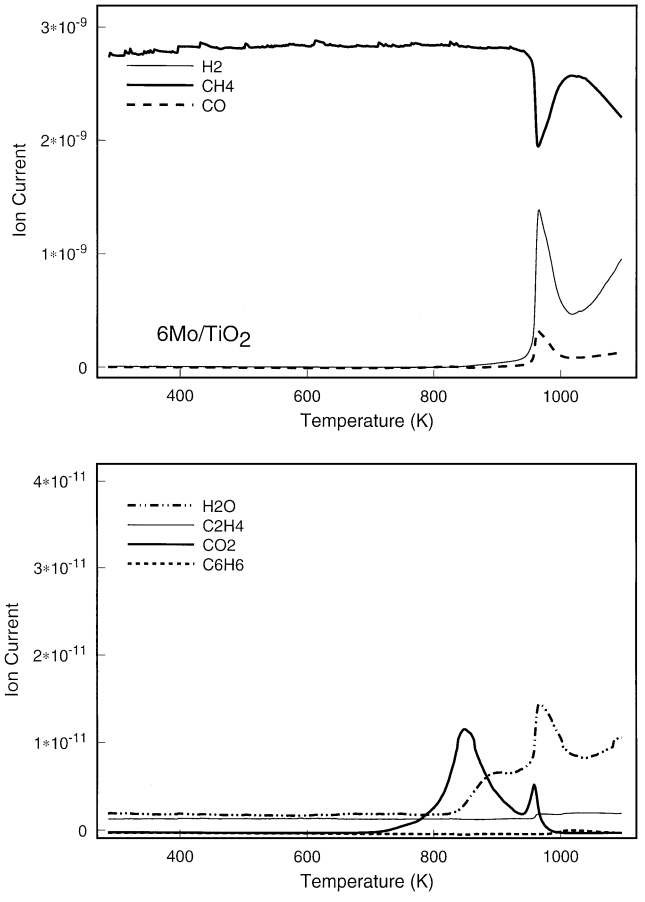

FIG. 9. TPSR profiles over the $6Mo/TiO_2$ catalyst. After the formation of molybdenum carbide, methane was still continuously consumed on the catalyst. However, no benzene production was observed.

mainly due to the carbonaceous deposits on the zeolite acid sites (8, 25), which retard the succeeding intermediate aromatization on these sites. However, the blocking of the Mo sites should also be considered, since it has been observed that some carbon did deposit on the Mo species. But, this in fact has no hindering effects on the smooth running of the reaction, since we have found that for the $6Mo/TiO_2$ catalyst, a continuous consumption of methane occurred even after the MoO_3 had transformed to Mo_2C. And also, the amount of CO_2 released in TPO is far greater than the amount of carbon in Mo_2C of $6Mo_2C/TiO_2$, if two molybdenum atoms associating with one carbon atom is considered (about 6 vesus 1). Thus, a multiple-layered carbon species must be formed on the molybdenum carbide surface. In other words, even though the multiple-layered carbon species remains on the surface of Mo_2C, gas-phase methane can still be activated on it. As the consequence, this leads to the appearance of the sharp peak in the TPO of 6Mo/HMCM-22 and $6Mo/TiO_2$ at 742 and 772 K, respectively. If there are Brønsted acid sites on the catalyst, the activated species will migrate to the acid sites and complete their aromatization, leaving the coke on the acid sites (the peak at 830 K in the TPO of 6Mo/HMCM-22). However, for the catalyst without Brønsted sites (Mo/TiO_2), such a phenomenon would not happen; then, only the peak corresponding to the carbonaceous deposits on molybdenum carbide would be observed. The formation of multilayered carbon species has already been reported for various supported or unsupported molybdenum carbide catalysts (24, 29), and it is taken as a general characteristic of molybdenum carbide catalysts. No similar situation has been observed in the cobalt carbide catalyst (see TPSR of Co/HMCM-22), and no benzene formation can be monitored even in the presence of the needed Brønsted acid sites.

The above discussion shows that molybdenum carbide is a good catalyst for methane aromatization. It can continuously activate methane even if it is covered by multilayered carbonaceous species. If MoO_3 is transformed into molybdenum carbide before the reaction, the formation of benzene would be observed as early as 847 K (we believe that the temperature could be further lowered if a more rigorous condition could be established). It is a combination of the special characteristics of the molybdenum carbide, the

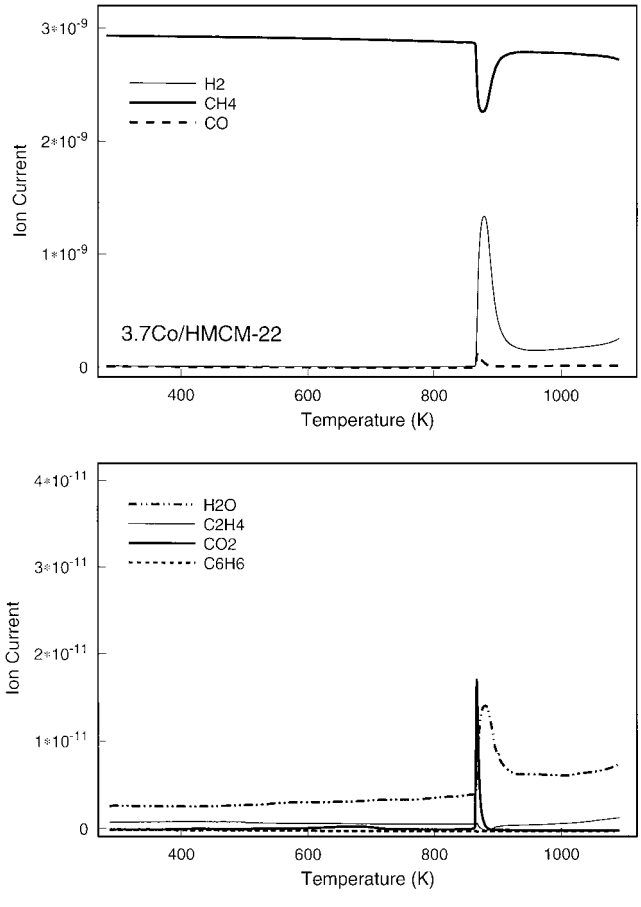

FIG. 10. TPSR profiles over the 3.7Co/HMCM-22 catalyst. At about 900 K, methane depletion ceased.

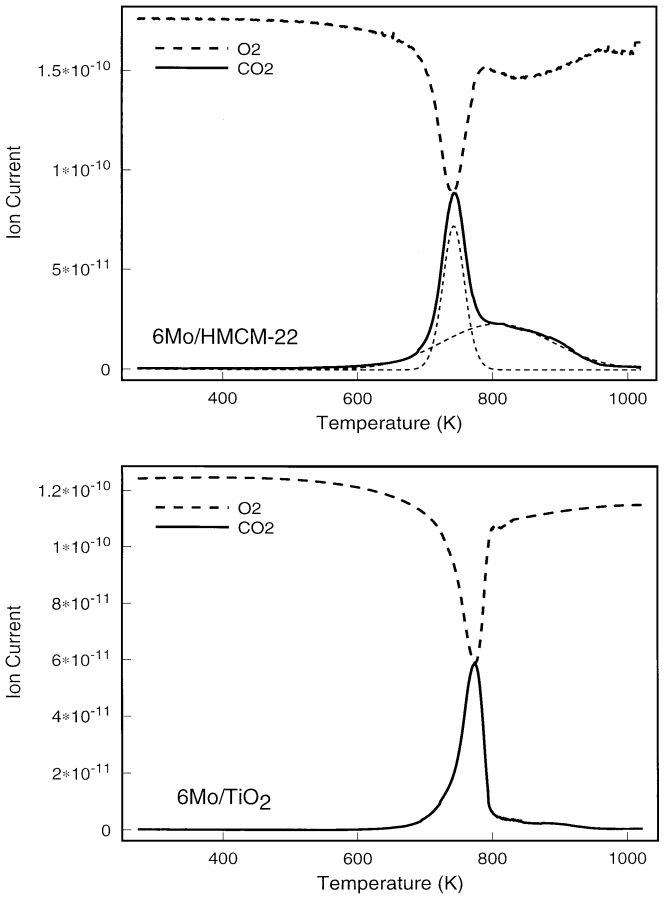

FIG. 11. TPO of the 6Mo/HMCM-22 and the 6Mo/TiO_2, both after 3 h of reaction (SV = 1500 ml/g · h). After cooling to RT in methane atmosphere, the samples were swept with 10% O_2/He at RT for 1 h before TPO began.

Brønsted acid sites, and the zeolite channel structure that is responsible for the outstanding performance of the catalyst in methane aromatization.

ACKNOWLEDGMENTS

The authors appreciate the support of the National Natural Science Foundation of China and the Ministry of Science and Technology of China. The kind donation of a mass spectrometer from the Alexander von Humbolat-Foundation is gratefully acknowledged.

REFERENCES

1. Crabtree, R. H., *Chem. Rev.* **95**, 987 (1995).
2. Koert, T., Deelen, M. J. A. G., and van Santen, R. A., *J. Catal.* **138**, 101 (1992).
3. Amariglio, A., Belgued, M., Pareja, P., and Amariglio, H., *J. Catal.* **177**, 113 (1998).
4. Krylov, O. V., *Catal. Today* **18**, 209 (1993).
5. Wang, L., Tan, L., Xie, M., Xu, G., Huang, J., and Xu, Y., *Catal. Lett.* **21**, 35 (1993).
6. Ono, Y., *Catal. Rev. Sci. Eng.* **34**, 179 (1992).
7. Schuurman, Y., Decamp, T., Pantazidis, A., Xu, Y. D., and Mirodatos, C., *Stud. Surf. Sci. Catal.* **109**, 351 (1997).
8. Wang, D., Rosynek, M. P., and Lunsford, J. H., *J. Catal.* **169**, 347 (1997).
9. Solymosi, F., Szoke, A., and Cserenyi, J., *Catal. Lett.* **39**, 157 (1996).
10. Zhang, J. Z., Long, M. A., and Howe, R. F., *Catal. Today* **44**, 293 (1998).
11. Ma, D., Shu, Y., Bao, X., and Xu, Y., *J. Catal.* **189**, 314 (2000).
12. Ma, D., Zhang, W., Shu, Y., Xu, Y., and Bao, X., *Catal. Lett.* **66**, 155 (2000).
13. Ohnishi, R., Liu, S., Dong, Q., Wang, L., and Ichikawa, M., *J. Catal.* **182**, 92 (1999).
14. Solymosi, F., Cserenyi, J., Szoke, A., Bansagi, T., and Oszko, A., *J. Catal.* **165**, 150 (1997).
15. Borry, R. W., III, Kim, Y. H., Huffsmith, A., Reimer, A., and Iglesia, I., *J. Phys. Chem. B* **103**, 5787 (1999).
16. Shu, Y., Ma, D., Bao, X., and Xu, Y., *Catal. Lett.* (submitted).
17. Rubin, M., and Chu, P., U.S. Patent 4 954 325, 1990.
18. Corma, A., Corell, C., and Pérez-Pariente, J., *Zeolites* **2**, 15 (1995).
19. Leonowicz, M. E., Lawton, J. A., Lawton, S. L., and Rubin, M. K., *Science* **264**, 1910 (1994).
20. Corma, A., *Microporous Mesoporous Mater.* **21**, 487 (1998).
21. Lee, J. S., Yeom, M. H., Park, K. Y., Nam, I.-S., Chung, J. S., Kim, Y. G., and Moon, S. H., *J. Catal.* **128**, 126 (1991); Leary, K. J., Michaels, J. N., and Stacy, A. M., *J. Catal.* **101**, 301 (1986).
22. Weckhuygen, B. M., Rosynek, M. P., and Lunsford, J. H., *Catal. Lett.* **52**, 31 (1998).
23. Solymosi, F., Erdohelyi, A., and Szoke, A., *Catal. Lett.* **32**, 43 (1996).
24. Miyao, T., Oshikawa, K., Omi, S., and Nagai, M., *Stud. Surf. Sci. Catal.* **106**, 255 (1997).
25. Xu, Y., Liu, S., Wang, L., Xie, M., and Guo, X., *Catal. Lett.* **30**, 135 (1995).
26. Mériaudeau, P., Tiep, L. V., Ha, V. T. T., Naccache, C., and Szabo, G., *J. Mol. Catal. A: Chemical* **144**, 469 (1999)
27. Oyama, S. T., *Catal. Today* **15**, 179 (1992).
28. Querini, C. A., and Fung, S. C., *Appl. Catal. A: General* **117**, 53 (1994).
29. Miyao, T., Shishikura, I., Matsuoka, M., Nagai, M., and Oyama, S. T., *Appl. Catal. A: General* **165**, 419 (1997).